

# Structure–Property Relationship in Fibers Spun from Poly(ethylene terephthalate) and Liquid Crystalline Polymer Blends. I. The Effect of Composition and Processing on Fiber Morphology and Properties

ZORAN S. PETROVIĆ<sup>1,\*</sup> and RICHARD FARRIS<sup>2</sup>

<sup>1</sup>Pittsburgh State University, Center for Design, Development and Production, Pittsburgh, Kansas 66762;

<sup>2</sup>Department of Polymer Science and Engineering, University of Massachusetts, Amherst, Massachusetts 01003

## SYNOPSIS

Poly(ethylene terephthalate) (PET) matrix was modified by blending with a specially prepared thermotropic liquid crystalline polymer (TLCP), in the hope to make the *in situ* composite during fiber spinning. It has been found that the TLCP did not fibrillate in the PET matrix at any concentration under given processing conditions, although it did in the polycarbonate matrix. This was explained by the low interaction parameter (low surface tension) and partial degree of mixing of PET and TLCP. The TLCP was an excellent processing aid even at very low concentrations, but it had an adverse effect on the strength of highly drawn fibers. The modulus of both undrawn and highly drawn fibers increases slightly with increasing TLCP concentration. © 1995 John Wiley & Sons, Inc.

## INTRODUCTION

Poly(ethylene terephthalate) (PET) is a semi-crystalline polymer that is widely used for synthetic fibers because of its excellent properties. Further improvement in the PET fiber properties can be accomplished by chemical modifications or by blending with other polymers. In this work, we attempted to improve mechanical properties of PET fibers, by blending PET with an immiscible thermotropic liquid crystalline polymer (TLCP). We investigated the possibility of obtaining *in situ*-reinforced PET matrix with TLCP. *In situ* composites are fiber-reinforced materials based on blends of two polymers, where one of the components forms fibers in the matrix of the other during processing. Fibrillation of one component during biphasic flow may not be obtained readily as it depends on many factors. One of the objectives of this work was to examine if our TLCP would

form *in situ* composites in a PET matrix and to study the effect of morphology on mechanical properties.

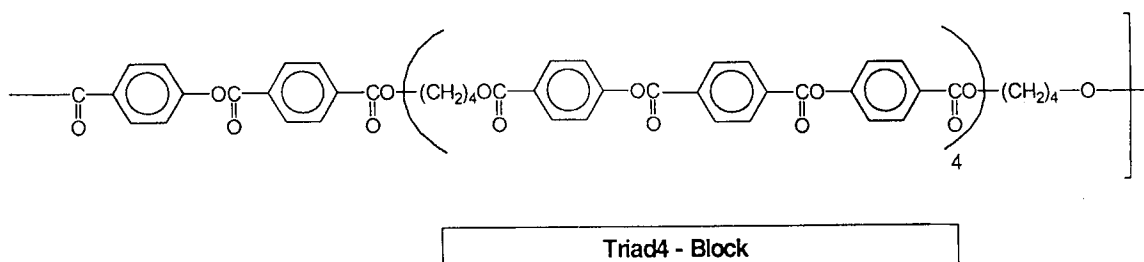
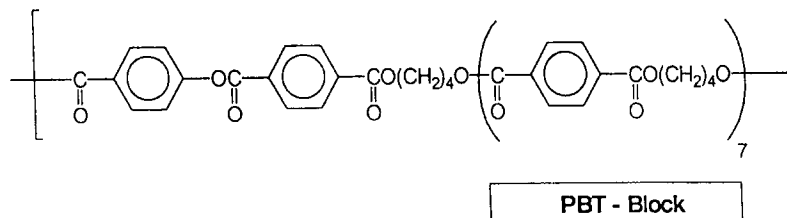
Fibrillation occurs only under special conditions that are dependent on rheological parameters such as the deformation rate and the viscoelastic properties of the matrix<sup>1–5</sup> as well as on the polymer–polymer interaction in the blend. It has been shown that the same TLCP, which was used in this work, fibrillated in the polycarbonate matrix.<sup>6</sup> A number of investigators reported recently *in situ* fibril formation during processing of biphasic blends containing a liquid crystalline polymer (LCP) component.<sup>7–9</sup> It appears that the largest single group of self-reinforcing composites was based on polycarbonate and various LCPs, which were prepared by extrusion, compression, and injection molding or fiber spinning.<sup>10–13</sup> The existence of fibrillation in blends of PET and various TLCPs was confirmed in some cases<sup>14,15</sup> and was inferred but not documented in others.<sup>16,17</sup> In several cases during film and rod extrusion, fibrillation of TLCP did not occur.<sup>18,19</sup> A wide range of morphologies and properties of PET/TLCP blends suggests that the control of the structure is a rather complex problem, influenced

\* To whom correspondence should be addressed at Pittsburgh State University, Center for Design, Development and Production, Pittsburgh, KS 66762.

by a number of parameters, all of which are not readily controllable.

Composite morphology of the biphasic fibers is characterized either by the globular or fibrillar shape of the dispersed phase. It is not clear what morphology is more favorable for fibers that have to be drawn to a high draw ratio. If rigid fibrils are undergoing the same degree of drawing as the PET

matrix, breaking of the TLCP phase and unpredicted effects on properties may be expected. Our work focused on the morphology and properties at low concentrations (up to 15%) of TLCP in the PET matrix, as well as on the effect of processing conditions on properties. The structure and synthesis of our LCP, designated as TR-4-co-PBT copolymer was described earlier.<sup>20</sup> Its structural formula is



Our investigation consisted of blending PET and TLCP and extruding fibers, which were posttreated (cold- and hot-drawn) in order to reach a high degree of crystallinity and orientation. Mechanical and thermal properties of the fibers were tested. Optical and electron microscopy was used to study the morphology of the fibers.

## EXPERIMENTAL

Fiber-grade PET was used as a matrix polymer. TR-4-co-PBT (2, 4, 7) liquid crystalline polymer was prepared using the previous synthetic scheme.<sup>20</sup> Inherent viscosity at the concentration 0.5 g/dL was found to be about 0.5. The properties and transitions in this TLCP were described earlier.<sup>21</sup>

### Methods

Polymer blends were prepared by tumble mixing ground PET and LCP, compression molding, and regrinding the blend, followed by drying in vacuum oven for at least 2 days. Extrusion of fibers was carried out in the custom-made miniature extruder, manufactured by Randcastle Extrusion Systems. Two fiber take-up speeds were used, 75 and 225 m/

min, producing typical diameters for the undrawn fibers of about 100 and 60 microns, respectively, which corresponded to the stretch ratio in the melt state of 250–700. The extruder had three heating zones: entry zone (1), two melting zones (2 and 3), and the die. Temperatures of the zones were 220, 260, 290, and 290°C, respectively. The concentrations of LCP in the PET/LCP blend were 0, 2.5, 5, 10, and 15%. An Olympus polarizing microscope, Model BHSP, linked to the video system was used for optical studies. A JEOL scanning electron microscope, Model 35 CF, was used to study fine morphological features of the fibers. An Instron tensile tester linked to a data acquisition system was used for mechanical studies. The sample length was 50 mm. The extension rate was 10%/min for cold-drawn or 200%/min for undrawn samples.

## RESULTS AND DISCUSSION

### The Effect of Processing Conditions on Morphology of Polymer Blends

Fibrillar morphology of *in situ* composites is closely related to the biphasic structure of the blend melt during flow. Deformation of the spherical droplet

suspended in a fluid during flow was first theoretically described by Taylor.<sup>1</sup> Apparent deformation,  $D$ , of the droplet into the ellipsoid and then the fiber was defined as

$$D = (L - S)/(L + S) \quad (1)$$

where  $L$  is the long axis, and  $S$ , the short axis of the ellipsoid. Apparent deformation is related to the Weber number,  $W_e$ , and the ratio of viscosities,  $k = \eta_d/\eta_m$ :

$$D = W_e[(19k + 16)/(16k + 16)] \approx W_e \quad (2)$$

where

$$W_e = (\eta_m \dot{\gamma} a)/\sigma \quad (3)$$

Here,  $\eta_m$  and  $\eta_d$  are the viscosities of the matrix and the dispersed phase, respectively;  $\dot{\gamma}$ , the shear rate;  $a$ , the droplet diameter, and  $\sigma$ , the interfacial tension between two fluids.

Thus, higher deformation is favored by higher viscosity of the medium and by higher shear rate and droplet size, while surface tension acts the opposite way. Schematic representation of the droplet deformation during elongation flow as a function of the flow rate is shown in Figure 1. Figure 1 shows schematically that by increasing the flow rate the droplet suspended in the matrix fluid changes its shape from sphere to ellipsoid to fiber, which eventually breaks up into smaller droplets. Breakup of the fiber [transition from (c) to (d)] occurs at a critical Weber number, which is the function of viscosity ratio,  $k$ .

The processing condition for the preparation of *in situ* composites should allow formation of fibers but not their breakup into smaller droplets. The stability condition, according to Tavgac,<sup>22,2</sup> is determined by the viscosity ratio,  $k$ . He found that in the uniform shearing flow stability region favorable conditions for fiber formation are roughly below  $k = 5 \times 10^{-3}$  and above about 5. According to Tse-brenko et al.,<sup>3</sup> fibrillation takes place at  $k \geq 1$ . However, we reported<sup>6</sup> fibrillation in polycarbonate/TLCP blends (the same TLCP as used in this work) where  $k$  was between 0.01 and 0.001.

An additional factor that may affect the fibrillation is the blend composition, i.e., the concentration of the dispersed phase in the matrix. Literature data on the effect of concentration of the dispersed phase on fibrillation are conflicting. Several authors<sup>5,7,8,18</sup> reported a change from discrete to fibrillar morphology as the LCP concentration in-

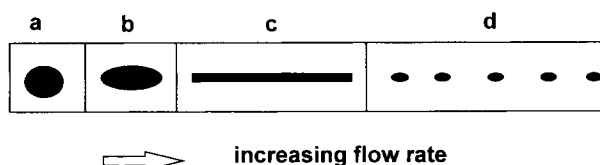


**Figure 1** Schematic representation of the droplet deformation in a liquid medium as a function of the flow rate.

creased above a certain critical concentration. Isayev and Modic,<sup>10</sup> however, found that fibrils were formed at a low LCP content and that at high concentration (above 25%) only dispersed domains are observed. Formation of fibrils at low concentrations of LCP was found also by other groups.<sup>6,19</sup> It appears that the effect of concentration is not unequivocal and that it depends on the system and conditions studied. We used a PET/LCP blend with approximately the same viscosity ratio as that of a polycarbonate/LCP blend that we reported earlier.<sup>6</sup> However, interfacial tension (which scales with interaction parameter) in PET/LCP is much lower than that in PC/LCP blends. It appears from previous considerations that deformation of a suspended LCP droplet in the PET melt should be much higher than in the PC matrix, all other conditions being the same.

### Miscibility of PET/TR-4-co-PBT Blends

Properties of a polymer blend depend largely on the degree of miscibility of the polymers. In many applications as well as in this one, two-phase morphology with strong interaction between phases is preferred. It has been demonstrated that even the pure LCP used in this work has the two-phase structure, characterized by separate melting points of the mesogen and PBT blocks. When TR-4-co-PBT(2, 4, 7) was blended with PET, a complex morphology resulted.

Miscibility of PET and TLCP was estimated from the calculated  $\chi$  parameter, which was found to be 0.011. This calculation is based on the group contribution method as explained in the Appendix. Miscibility of two polymers occurs when the  $\chi$  parameter is lower than  $\chi_{\text{critical}}$ . The critical value of  $\chi$  depends on molecular weight (or degree of polymerization,  $x$ ) of both components according to the relationship

$$\chi_{\text{crit}} = 0.5(1/x_1^{0.5} + 1/x_2^{0.5})^2 \quad (4)$$

For infinite (or very large) molecular weights,  $\chi_{\text{crit}}$  becomes zero. To obtain miscibility, a negative value of the interaction parameter is required, e.g., specific

interactions, such as hydrogen bonding, acid–base, donor–acceptor, etc., should be present. Miscibility may not be achieved even if these enthalpic requirements are met, due to unfavorable entropic conditions caused by the excessive rigidity of one of the components, as in the case of liquid crystalline components. In our case, in spite of very close solubility parameters and small  $\chi$  parameter, two components were immiscible as observed from separate melting points of the two components. Some degree of miscibility was present, possibly due to the miscibility of PET and PBT blocks from the TLCP copolymer. Miscibility and properties of the PET/TR-4-co-PBT blends will be discussed in a separate article.<sup>23</sup> It was difficult to separate components by dissolution because of the high degrees of structural dissolution and of structural similarity and the partial mixing of the two phases. That also made contrasting in electron microscopy difficult.

### Morphology of PET/TLCP Fibers

The main body of the work discussed here was carried out on samples spun under “standard” conditions, i.e., using the following extruder temperature scheme: zone 1 (entrance), 220°C; zone 2, 260°C; zone 3, 290°C; and die temperature, 290°C and take-up speeds of 75 and 225 m/min. All our attempts to find evidence of continuous fibrils of the dispersed LCP phase in the PET matrix were inconclusive. Brittle fracture of the fibers occurred while stretching them quickly in liquid nitrogen. Electron micrographs of the fractured surface of the as-spun neat PET and PET/10% LCP fibers, produced at the take-up speed of 75 m/min, are shown on Figures 2 and 3.

The concentric circles on the as-spun PET [Fig. 2(a)] reflect flow layers of the melt but no specific features were observed. At magnification of 10,000 times [Fig. 2(b)], some roughness of the surface was observed. However, the fractured surface of the fiber containing 10% LCP, as Figure 3(a) and (b) show, is much more irregular even at lower magnification, with some globular features.

Apparently, very little happens with the morphology after cold- and hot-drawing of PET and PET/LCP fiber. Figure 4(a) exposes the rough fracture surface of the hot-drawn PET fiber, and Figure 4(b), the same for the hot-drawn PET/10% LCP fiber. Although the matrix become oriented, it appears that there is little chance to deform significantly the dispersed globular phase. Figure 4(b) suggests that the prevailing morphology of the LCP phase in the PET/LCP fiber is probably globular.

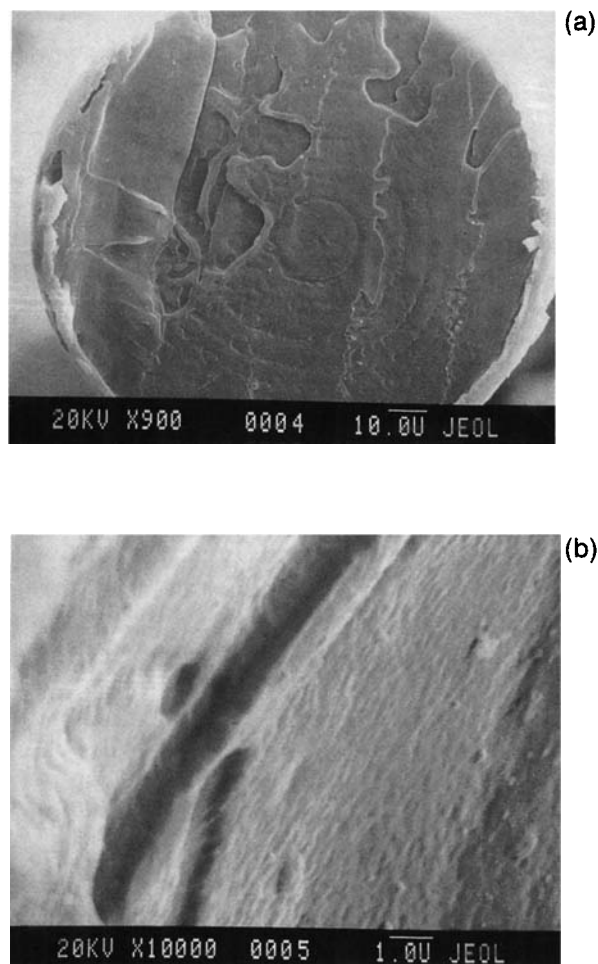


**Figure 2** Electron micrographs of the fracture surface of the as-spun PET fiber at two magnifications: (a) 900 $\times$  and (b) 10000 $\times$ .

Figures 3 and 4(b) reveal little information on the possible morphology of the dispersed phase, possibly due to good mixing of the two phases and a low contrast coming from the structural similarities of the phases. Unexpectedly, clearer insight into the morphology came from the optical microscopy. The fiber containing 10% LCP was embedded in the epoxy resin, and upon solidification, cut longitudinally using a microtome. Figure 5(a) and (b) shows reflected light optical micrographs of the sections of the longitudinally microtomed fibers embedded in epoxy resin. At a very high magnification [Fig. 5(a)], it is possible to observe whitish spots, not larger than a micron, in two fibers. Figure 5(b) shows a not so cleanly microtomed fiber, because the knife was not completely parallel to the fiber axis. White inclusions in this case were not necessarily round and some relatively large chunks of the dispersed phase are observed. It is not clear if this morphology

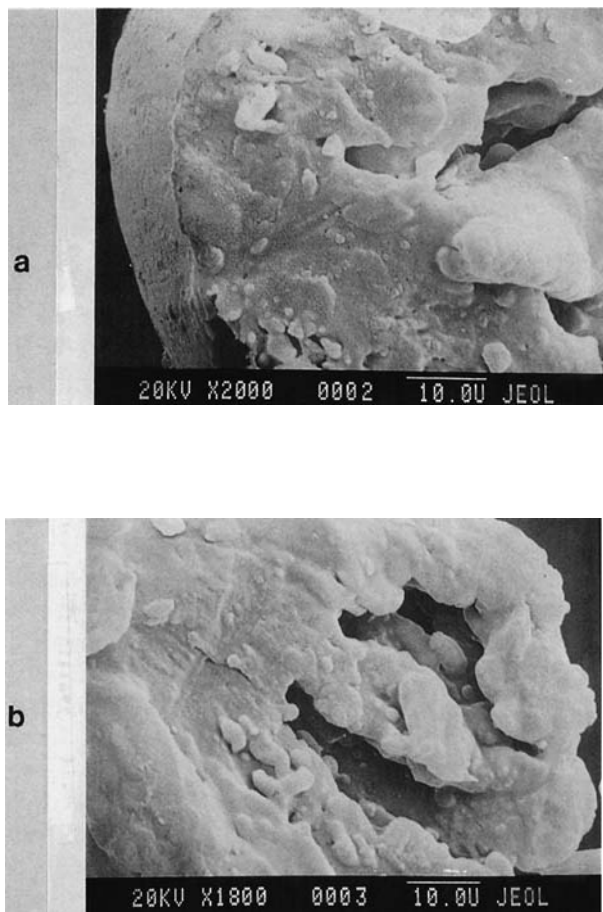


**Figure 3** Electron micrographs of the fracture surface of the PET/10% LCP fiber at two magnifications: (a) 2000 $\times$  and (b) 1800 $\times$ .

is representative of all fibers. In conclusion, we did not see any indication of fibrillar morphology, although it was shown that the same LCP does fibrillate in the polycarbonate matrix under the same processing conditions.<sup>6</sup>

#### Effect of LCP Concentration on Properties

Rheological properties measured during cooling of the pure PET and PET containing 2.5% LCP and 5% LCP are displayed in Figure 6. Complex viscosity of the LCP was about three orders of magnitude lower than that of PET. A jump in complex viscosity of LCP upon cooling was observed at about 250°C, while that limit for PET was found around 220°C. Addition of only 2.5% of LCP to PET reduced the viscosity of the melt by about three times, indicating that this TLCP is an excellent processing aid. Lower viscosity of the blends containing higher TLCP is reflected in a somewhat larger diameter fibers, since

the output of the extruder was controlled by the number of screw rotations which was generally kept constant and viscosity of the melt which was not controlled. Fiber diameters were measured using an optical microscope connected to the TV screen and VCR-printer. As-spun fibers were cold drawn at about 75°C and then hot-drawn at about 200°C. Draw ratio ( $DR$ ) was calculated from the reduction in diameter of the fiber before and after drawing ( $DR = D^2/d^2$ ). The results of tensile tests are the average of nine measurements. Standard deviation in all tests was lower than 10% except in the elongation at break of as-spun fibers, where the relative error could be larger.

Figure 7 shows the variation of the modulus of as-spun fibers obtained at two take-up speeds. It illustrates the fact that increasing LCP content slightly increases the modulus of the as-spun fibers. It will be shown that the same level of modulus of as-spun PET fibers as that of PET/LCP fibers can be easily obtained by altering spinning tempera-

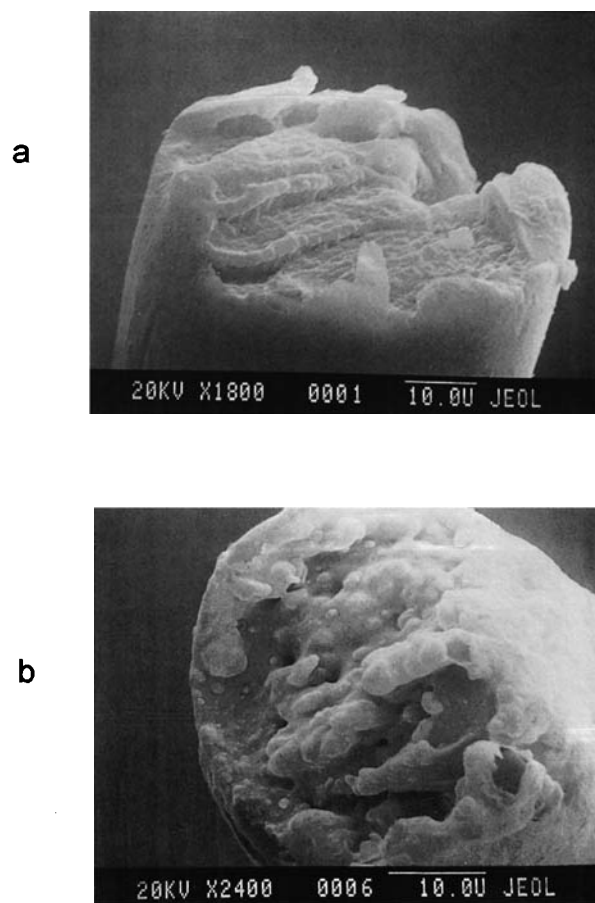


**Figure 4** Electron micrographs of the fractured hot-drawn (a) PET and (b) PET/10% LCP fiber.

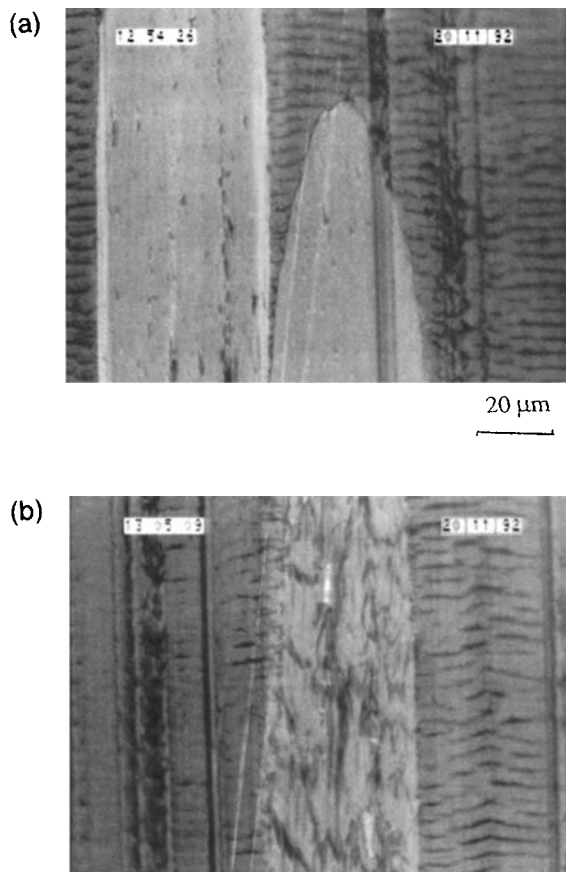


**Figure 5** Reflected light optical micrograph of the microtomed PET/10% LCP fiber: (a) two microtomed, hot-drawn fibers ( $d \sim 20 \mu\text{m}$ ) embedded in epoxy matrix; (b) microtomed, hot-drawn fiber ( $d \sim 26 \mu\text{m}$ ) embedded in epoxy matrix.

ture.<sup>24</sup> Since the modulus is very sensitive to orientation, crystallization conditions during spinning and resulting orientation determine how high the

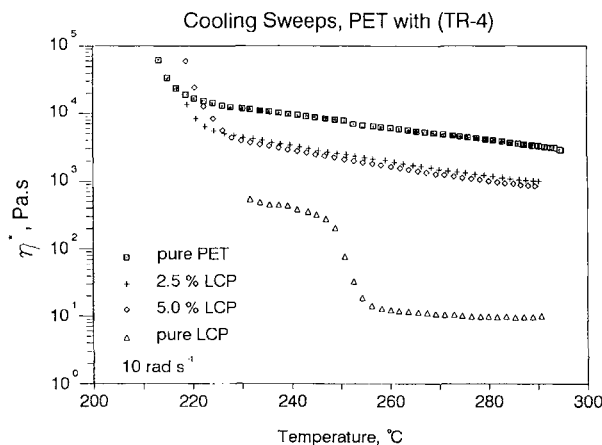


**Figure 6** Change of complex viscosity with temperature of pure PET, LCP, and their blends.

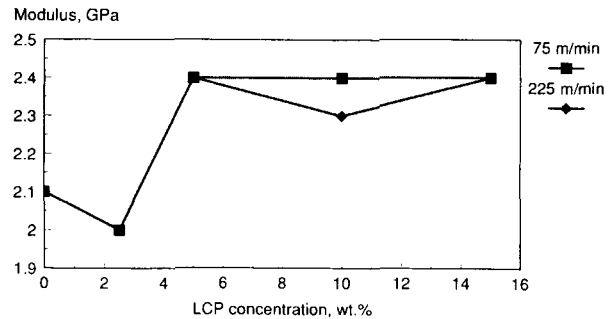


**Figure 7** Effect of LCP concentration on modulus of as-spun fibers obtained at two take-up speeds.

modulus will be. It is likely that matrix modification due to the addition of LCP affects the modulus more than the mixture rule predicts. The modulus of the hot-drawn fibers (Fig. 8) increased significantly only after addition of 15% of LCP, although the total increase was not greater than 10%. As will be shown later, the addition of 10% LCP helps increase the modulus about 10% when spun at higher temperature. Take-up speed may have some effect on crystallization conditions as faster cooling, due to a lower diameter of fibers spun at 225 m/min, occurs. However, no significant effect of the take-up speed on the modulus was observed in as-spun fibers. Somewhat higher draw ratios could be attained in thicker fibers (spun at 75 m/min), resulting in higher orientation and, thus, higher moduli of these fibers. All results are obtained at the highest attainable draw ratios, which varied from sample to sample.

A good measure of the draw ratio can be obtained from the results of elongation at break. Elongation at break is about 7%. Higher values indicate that the fiber was not drawn to a maximum, resulting in somewhat lower moduli and strengths.

Tensile strengths of as-spun fibers vs. concentration of LCP are given in Figure 9. This property in as-spun fibers is not technically important. It does,

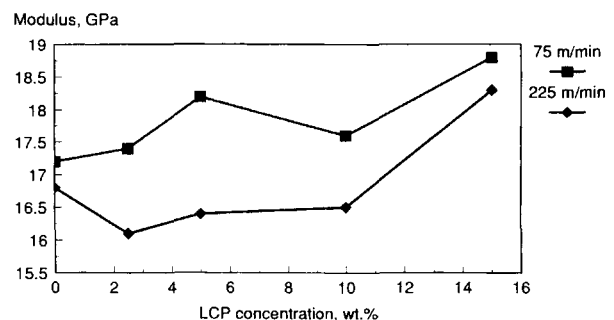


**Figure 8** Effect of LCP concentration on modulus of hot-drawn fibers.

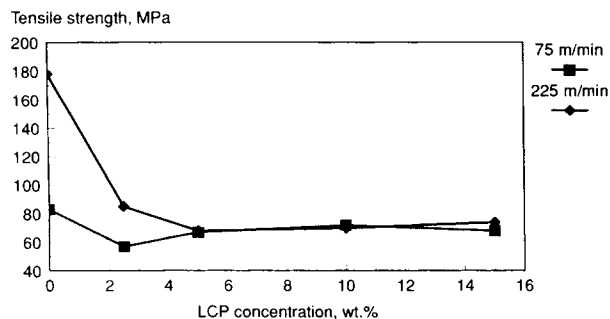


**Figure 9** Tensile strength of as-spun PET/LCP fibers vs. LCP concentration.

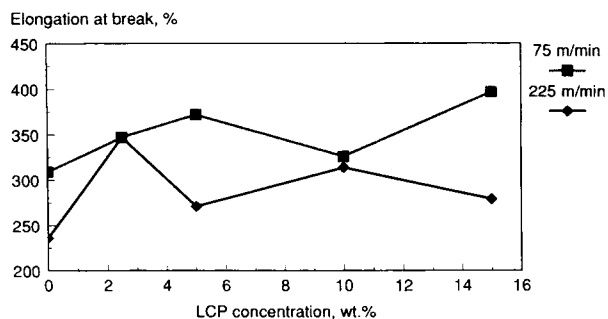


**Figure 11** Elongation at break of as-spun fibers vs. LCP concentration.

however, reflect changes in crystallization and orientation states of the fiber during cold drawing, occurring during the tensile test. It is noteworthy that this property was virtually independent of LCP concentration, except for neat PET fiber obtained at a take-up speed of 75 m/min.

Tensile strength of the hot-drawn fibers appears, as Figure 10 shows, to be impaired by the presence of the LCP phase. It suggests that the LCP phase acts as a defect in the oriented PET matrix. It should be emphasized that the LCP used was of fairly low molecular weight and could not be tested in the pure state.

Elongation at break of as-spun fibers is a measure of attainable cold drawing at the test temperature. It appears that addition of the LCP allows higher draw ratios than in the neat PET fiber, although this dependence is not clearly defined, as Figure 11 shows. Elongation at break of hot-drawn fibers was between 7 and 8%, indicating near optimal draw ratios.

**Effect of Drawing Temperature on Properties**

Cold drawing of polymers is usually carried out slightly below the glass transition temperature. We varied this temperature from 70 to 90°C (glass transition of PET is about 75°C) without a consequence

on the draw ratio. The effect of temperature used in hot drawing is of much greater significance. In our work, fiber was in contact with the surface of the hot plate with controlled temperature during the drawing process. Two fibers, one based on neat PET and another based on PET/15% LCP, were each hot-drawn at three temperatures and the effect of drawing temperature on properties examined. Hot drawing is carried out at temperatures near the melting of PET. We used 215, 177, and 143°C for PET and 235, 210, and 162°C for PET/15% LCP. It should be emphasized that elongation at break in all cases was around 7%, indicating an optimal draw ratio. The effect of drawing temperature on the modulus of PET and PET/15% LCP fibers is displayed in Figure 12. Figure 12 reveals that differences in moduli of the fibers drawn at three temperatures are within experimental error, indicating little influence of drawing temperature on modulus. The effect of drawing temperature on tensile strength of PET and PET/15% LCP fibers (Fig. 13) was not significant in the range of temperatures used. All variations were within the limits of experimental error.

An important reason for incorporating LCP in the matrix of a thermoplastic polymer is to reduce

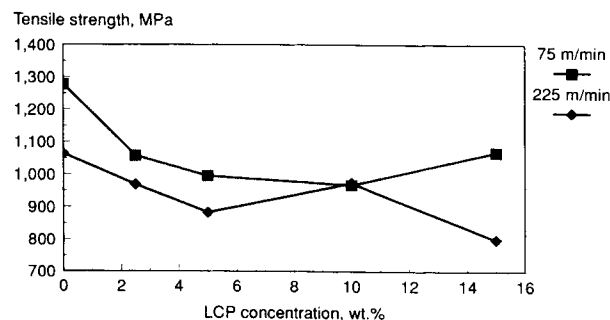


**Figure 10** Tensile strength of hot-drawn PET/LCP fibers vs. LCP concentration.

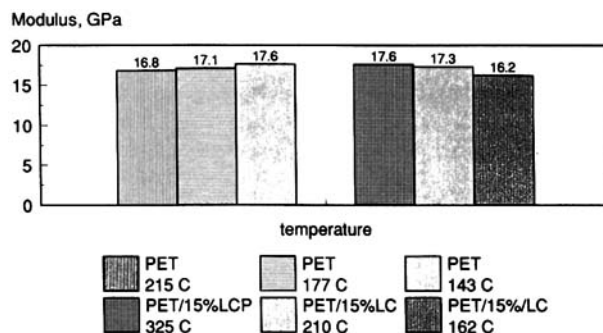


**Figure 12** The effect of temperature of drawing on modulus of hot-drawn PET and PET/15% LCP fibers.

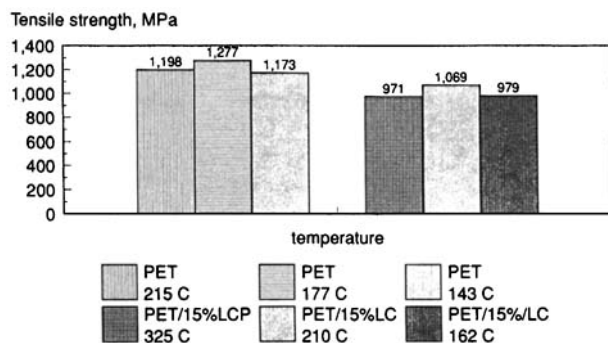


**Figure 13** Effect of drawing temperature on tensile strength of PET and PET/15% LCP fibers.

thermal shrinkage. Thermal shrinkage is tested by heating a fiber for 15 min at 190°C, conditioned previously for 24 h at 65% relative humidity and at room temperature. Figure 14 shows that the effect of drawing temperature on shrinkage is significant. At drawing temperatures above the shrinkage test temperature (190°C), the structure is fixed by high melting crystallites, resulting in reduced shrinkage. If drawing temperatures are below that of the shrinkage test, shrinkage is considerable, being higher in samples drawn at a lower temperature. Thus, drawing temperature is primarily affecting thermal shrinkage.

## CONCLUSIONS

A series of fibers based on poly(ethylene terephthalate) (PET) and TR-4-co-PBT (2, 4, 7) liquid crystalline polymer (LCP) were prepared and the effect of concentration and spinning temperature on morphology and properties examined. It was found that this particular LCP has a very close solubility parameter to that of PET and that resulting morphology of the dispersed phase was never fibrillar, unlike the case of the same LCP and polycarbonate.

The modulus of both undrawn and hot-drawn fibers increases slightly with the increasing LCP concentration, but the modulus of the pure LCP phase, which could not be tested in the form of fibers, was not much higher than that of the PET itself. The properties of fibers based on PET/LCP blends are thought to be affected by the matrix modification in the presence of LCP. Moduli of fibers based on blends were slightly increasing and tensile strengths decreasing with increasing LCP concentration. The effect of drawing temperature was reflected in increased thermal shrinkage if drawing temperatures were below the shrinkage test temperature, but it had little influence on modulus and tensile strength.

## APPENDIX

Interaction parameter,  $\chi$ , can be calculated from known solubility parameters,  $\delta$ , of the components in the binary mixture, using the expression

$$\chi = \frac{(\delta_1 - \delta_2)^2 V_1}{RT}$$

where  $\delta_1$  and  $\delta_2$  are solubility parameters of the two components, and  $V_1$ , the molar volume of the solvent or repeat unit of the polymer. Conveniently, the value of  $V_1 = 100 \text{ cm}^3/\text{mol}$  is taken for polymer mixtures.  $R$  is the gas constant, and  $T$ , the temperature.

Solubility parameters can be estimated from the chemical structure of the polymers using molar attraction constants,  $F_i$ , and molar volumes of the corresponding chemical groups,  $V_i$ :

$$\delta = \frac{\sum F_i}{\sum V_i}$$

Values of  $F_i$  and  $V_i$  for various chemical groups are given in tables below.<sup>25,26</sup>

### Calculation of $\delta_{\text{PET}}$

The repeat unit of PET has

	$F_i$ [(MPa) <sup>1/2</sup> cm <sup>3</sup> /mol]	$V_i$ (cm <sup>3</sup> /mol)
2 —CO—O—	$682 \times 2 = 1364$	$24.6 \times 2 = 49.2$
—C <sub>6</sub> H <sub>4</sub> —(Ar)	1440	65.5
2 —CH <sub>2</sub> —	$269 \times 2 = 538$	$16.32 \times 2 = 32.6$
	$\Sigma F_i = 3342$	$\Sigma V_i = 147.3$
	$\delta_{\text{PET}} = 3342/147.3 = 22.7 \text{ (MPa)}^{1/2}$	

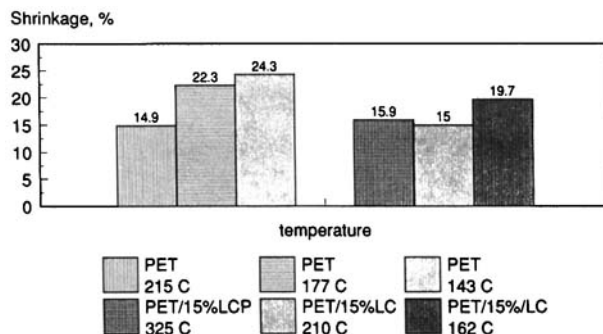


**Figure 14** The effect of drawing temperature on thermal shrinkage of PET and PET/15% LCP fibers.



The table value for PET (Van Krevelen) is 22.69, which is in excellent agreement with the calculated value. A range of experimental values from 19.9–21.9 was reported (Van Krevelen).

#### Calculation of $\delta$ Parameter for TR-4 co PBT

The TR-4/PBT [2,4,7] copolymer consists of

2 Diads	$\Rightarrow F_1 = 9888$	$V_1 = 409.6$
2 Butylene units	$\Rightarrow F_2 = 2152$	$V_2 = 131$
4 TR-4 units	$\Rightarrow F_3 = 32,592$	$V_3 = 1440.$
7 PBT units	$\Rightarrow F_4 = 27,244$	$V_4 = 1260$

$$\Sigma F_i = 71,876 \quad \Sigma V_i = 3241$$

$$\delta_{LCP} = 22.2 \text{ (MPa)}^{1/2}$$

$$\chi_{PET/LCP} = \frac{(22.7-22.2)^2 \times 100}{8.314 \times 298} = 0.011$$

#### REFERENCES

- G. I. Taylor, Proc. R. Soc. A, **146**, 501 (1934).
- C. D. Han, *Multiphase Flow in Polymer Processing*, Academic Press, New York, 1981, Chaps. 4 and 5.
- G. V. Vinogradov, B. V. Yarlykov, M. V. Tsebrenko, A. V. Yudin, and T. I. Ablazova, *Polymer*, **16**, 609 (1975).
- H. B. Chin and C. D. Han, *J. Rheol.*, **23**, 557 (1979).
- G. Crevecoeur and G. Groeninckx, *J. Appl. Polym. Sci.*, **49**, 839 (1993).
- Z. Petrović and R. Farris, to appear.
- G. Crevecoeur and G. Groeninckx, *Polym. Eng. Sci.*, **30**(9), 532 (1990).
- K. G. Blizard and R. R. Haghghat, *Polym. Eng. Sci.*, **33**(13), 799 (1993).
- D. Dutta, H. Fruitwala, A. Kohli, and R. A. Weiss, *Polym. Eng. Sci.*, **30**(17), 1005 (1990).
- A. I. Isayev and M. J. Modic, *Polym. Compos.*, **8**, 158 (1987).
- A. Kohli, N. Chung, and R. A. Weiss, *Polym. Eng. Sci.*, **29**(9), 573 (1989).
- D. Beery, S. Kenig, A. Siegman, and M. Narkis, *Polym. Eng. Sci.*, **32**(1), 14 (1992).
- Q. Lin, J. Jho, and A. F. Yee, *Polym. Eng. Sci.*, **33**(13), 789 (1993).
- B. Y. Shin, S. H. Jang, I. J. Chung, and B. S. Kim, *Polym. Eng. Sci.*, **32**(1), 1533 (1991).
- A. K. Mithal, A. Tayebi, and C. H. Lin, *Polym. Eng. Sci.*, **31**, 1533 (1991).
- E. Joseph, G. L. Wilkes, and D. G. Baird, *Polymer*, **26**, 689 (1985).
- S. Mehta and B. L. Deopura, *Polym. Eng. Sci.*, **33**(14), 931 (1993).
- A. M. Sukhadia, D. Done, and D. G. Baird, *Polym. Eng. Sci.*, **30**(9), 519 (1990).
- N. Chapeau, P. J. Careau, C. Peleteiro, P. A. Lavoie, and T. Malique, *Polym. Eng. Sci.*, **32**(24), 1876 (1992).
- F. Ignatious, S. W. Kantor, and R. W. Lenz, *Polym. Prepr.*, **34**(2), 586–587 (1993).
- R. Giesa, S. Joslin, D. Melot, and R. Farris, to appear.
- C. D. Han, *Multiphase Flow in Polymer Processing*, Academic Press, New York, 1981, p. 228, Fig. 5.2.
- D. Melot, Z. S. Petrović, A. Waden, and W. J. MacKnight, to appear.
- Z. Petrović and R. Farris, *J. Appl. Polym. Sci.*, **58**, 1349 (1995).
- D. W. Van Krevelen, *Properties of Polymers*, Elsevier, Amsterdam, 1990.
- J. Brandrup and E. H. Immergut, Eds., *Polymer Handbook*, Wiley, New York, 1989, p. VII-519.

Received February 23, 1995

Accepted May 17, 1995